

Laser spectroscopy of narrow doubly excited autoionizing states of ytterbium atoms

G. I. Bekov, E. P. Vidolova-Angelova, L. N. Ivanov, V. S. Letokhov, and V. I. Mishin

Institute of Spectroscopy, Academy of Sciences of the USSR, Moscow

(Submitted 27 May 1980)

Zh. Eksp. Teor. Fiz. 80, 866–878 (March 1981)

An analysis is made of doubly excited autoionizing states of an atom with two valence electrons. The results of experimental and theoretical investigations of narrow autoionizing states are reported for ytterbium atoms near the ionization threshold. The method of multistage photoionization of atoms by tunable laser radiation was used to detect experimentally and identify narrow autoionizing states ${}^1P_1^0$ and ${}^3P_{0,1,2}^0$ of the $7s6p$ configuration. The positions and widths of the autoionizing states belonging to the $7s6p$, $6p5d$, $6p^2$, and $5d^2$ configurations were calculated.

PACS numbers: 32.80.Dz

1. INTRODUCTION

Autoionizing states of complex atoms are attracting increasing interest. This is due to their potential applications in laser spectroscopy methods.

An autoionizing state is a bound state of an atom which lies above the ionization threshold of the outer valence electron. Such states appear in atoms usually as a result of excitation of inner shells. However, in the case of many-electron atoms the so-called shift terms form as a result of simultaneous excitation of two or more valence electrons. In the case of sufficiently strong excitation, one can then have configurations in which levels lie above the ionization threshold for one-electron excitation, i.e., such levels can also be of the autoionizing type. Since above the ionization threshold there are states in the continuous spectrum adjoining this threshold, there is a probability that an atom excited to a discrete state of energy higher than the ionization potential is transferred from this state to the continuum and is thus ionized. This is the essence of the phenomenon of autoionization.

Clearly, autoionizing states can decay in two ways: radiatively or nonradiatively, i.e., by autoionization involving the loss of an electron. The possibility of autoionization reduces the lifetime of a discrete state and broadens the state. Since autoionization can be regarded as a consequence of the superposition of the states in the continuous and discrete spectra, the probability of autoionization decay increases on increase in the coupling between the autoionizing state in question and the continuum.

Autoionizing states investigated up to now by the methods of classical spectroscopy have widths ($\Gamma \approx 10\text{--}100 \text{ \AA}$) much greater than the natural width of discrete states. In some cases this width can be 1 \AA , whereas the natural width of the discrete states is of the order of 10^{-4} \AA .

The development of laser spectroscopy methods, particularly that of multistep photoionization of atoms by laser radiation, has made it possible to carry out systematic investigations of autoionizing states in many-electron atoms which have a complex spectrum of bound states. A selection of different intermediate ex-

iting transitions in this method makes it possible to study autoionizing states of different parity. In the case of classical spectroscopy of the absorption spectra of atoms one can study only autoionizing states linked to the ground state of an atom, i.e., those with a parity opposite to that of the ground state and with a total momentum satisfying the selection rules for the optical transition in question. Moreover, laser spectroscopy methods extend considerably the opportunities for investigating very narrow autoionizing states which are important in many applications. Examples of these are the long-lived autoionizing states (lifetime about 0.5 nsec, $\Gamma \approx 0.05 \text{ cm}^{-1}$) of the Gd atom.¹ Up to now, relatively narrow autoionizing states have been observed for atoms of rare gases Ar, Kr, and Xe ($\Gamma \approx 10 \text{ cm}^{-2}$ —Ref. 2), alkaline earth elements such as the barium atom ($\Gamma \approx 10 \text{ cm}^{-1}$ —Ref. 3), the uranium atom ($\Gamma \approx 0.5 \text{ cm}^{-1}$ —Ref. 4), and some lanthanides ($\Gamma \approx 1\text{--}2 \text{ cm}^{-1}$ —Ref. 4), and some lanthanides ($\Gamma \approx 1\text{--}2 \text{ cm}^{-1}$ —Ref. 5). These ionizing states exhibit a scatter of widths within one or two orders of magnitude and some tendency for the reduction in the width in the case of heavier atoms.

Narrow autoionizing states are of interest not only from the point of view of the physics of many-electron atoms but are useful in schemes for selective multistep photoionization of atoms by laser radiation. The cross section for the excitation of an atom to a narrow autoionizing stage may reach a value of 10^{-15} cm^2 (Ref. 1), which is several orders of magnitude greater than the cross section for direct autoionization to the continuum. This makes it possible to achieve the maximum (unity) absolute yield in elementary quantum processes, which is extremely important in such tasks as laser detection of single atoms,⁶ isotope separation,⁷ and generation of intense photoion beams.

The present paper reports the results of experimental and theoretical investigations of such narrow autoionizing states near the ionization threshold of the ytterbium atom. This atom has, on the one hand, a complex many-electron system, and, on the other, a quantum system relatively simple for theoretical description.

2. QUALITATIVE ANALYSIS

We shall consider an atom of ytterbium whose ground electronic configuration is $4f^{14}6s^2$ and whose atomic

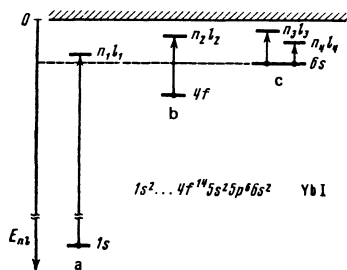


FIG. 1. Formation of autoionizing states of different types: a) excitation of a K shell, $|E(n_1 l_1) - E(1s)| > |E(6s)|$; b) excitation of a $4f$ shell, $|E(n_2 l_2) - E(4f)| > |E(6s)|$; c) double excitation of a valence shell, $|E(n_3 l_3) - E(6s)| + |E(n_4 l_4) - E(6s)| > |E(6s)|$.

number is $Z = 70$ (in this case, the $5s^2$ and $5p^6$ shells have a stronger binding than the $4f^{14}$ shell). We shall find two main types of autoionizing states for this complex atom. States of the first type appear on excitation of the inertials, whereas those of the second type appear as a result of double excitation of the valence shell. The autoionizing states resulting from the excitation of the $4f$ shell are of intermediate type. We shall describe qualitatively the states of the first and second types using the one-particle approximation. For states of the first type this is justified by the dominant role of the nuclear potential in the intraatomic region compared with the electron-electron interaction. In the case of the doubly excited valence shell the one-particle approximation is justified by the relatively large distance of this shell from the core.

Figure 1 shows schematically the excitation of all types of autoionizing state. The ordinate gives the electron energy in the one-particle approximation. The ionization threshold is labeled by 0. The excitation energy for an autoionizing state originating from an excited K shell (Fig. 1a) or from an excited $4f$ shell (Fig. 1b) should be sufficient for the detachment of a $6s$ valence electron. Autoionizing states appear as a result of double excitation of the valence shell (Fig. 1c) if the total energy of the valence electrons exceeds the ionization energy.

Autoionization decay can be represented as follows in the one-particle approximation: $\alpha_1 \alpha_2 \rightarrow \alpha_3 k$, where α_i ($i = 1, 2, 3$) describes the set of quantum numbers of the bound states and k is a free-electron state. The decay is then possible only to a state in the continuous spectrum which has the same parity and the same total momentum as the initial autoionizing state.

The level width Γ related to autoionization decay is governed by its coupling to states in the continuous spectrum:

$$\Gamma = 2\pi |\langle i | \hat{V} | f \rangle|^2 \propto |V(\alpha_1 \alpha_2, \alpha_3 k)|^2, \quad (1)$$

where $|i\rangle$ is the initial state of the system and $|f\rangle$ is the final state; \hat{V} is the electron-electron interaction operator. We shall use the Coulomb units. In the case of energy 1 Coulomb unit is $219476Z^2 \text{ cm}^{-1}$, where Z is the nuclear charge. The matrix element $V(\alpha_1 \alpha_2, \alpha_3 k)$ is governed by the overlap and relative positions of the

nodes of one-electron orbitals α_1, k and α_2, α_3 , respectively.

We shall consider the $1s[\dots]4f^{14}6s^2nl$ state with a K vacancy. This is the limiting case of states of the first type. Decay of this state is known as the Auger effect, when an electron from one of the nearest shells is transferred to the state $1s$ and at the same time one of the atomic electrons is injected. The main channels of the decay of this autoionizing state with a K vacancy are: $2s^2 - 1sks$, $2s2p - 1skp$ and $2p^2 - 1skl$. Similar two-electron processes have been investigated in the case of multiply charged ions of an He-like isoelectronic series.⁸ The radial part of the matrix element (1) is retained, to within quantities of the order of $1/Z$, when He-like ions are replaced with a many-electron system. Allowance for additional (passive) electrons in this approximation governs only the angular coefficients of the radial integrals. Therefore, in both cases a typical width of an autoionizing state is of the same order of magnitude and amounts to 10^8 cm^{-1} . In the case of some autoionizing states of He-like ions the decay is forbidden in the nonrelativistic approximation and these states are characterized by a relatively small width. There is no such forbiddenness in the case of states with a vacancy in an inner shell of a complex atom.

We shall now analyze low-lying autoionizing states of an atom of Yb which appear as a result of double excitation of the $6s^2$ shell. These states decay in accordance with the scheme $n_1 l_1 n_2 l_2 - 6skl$. We shall assume that the valence electrons move in a potential well formed by the core. The core is defined as the atomic nucleus together with all the inner electron shells, including the $4f$ shell. The interaction of the valence electrons is regarded as a perturbation. The experimental results are used to find one-electron energies of the valence electrons and the energy of their interaction. These quantities can be used to estimate the depth and size of the potential well. It follows from an analysis of the experimental spectra of the atoms of Ca, Ba, and Yb (Ref. 9) that the size of the well depends weakly on the nuclear charge Z but the depth of the well is proportional to Z . The region of localization of the valence electrons is governed by the size of the potential well. It would seem that the overlap of the electron orbitals should then vary little from atom to atom. However, as atoms become more complicated, the principal quantum numbers n_1, n_2, n_3 of the valence electrons increase and, consequently, there is an increase in the number of oscillations of the radial orbitals in the main electron localization region under consideration. This reduces the matrix element (1). We shall consider the case of a rectangular potential well of depth Z . The number of radial function nodes $\alpha_1, \alpha_2, \alpha_3$ is proportional to the principal quantum numbers n_1, n_2, n_3 . In the case of complex atoms we find that n_1, n_2 and n_3 are all proportional to $Z^{1/2}$.

We shall calculate the matrix element (1) under the same assumptions, which gives the qualitative estimate

$$\Gamma \propto 1/Z^2. \quad (2)$$

An approach of this kind utilizing the one-particle

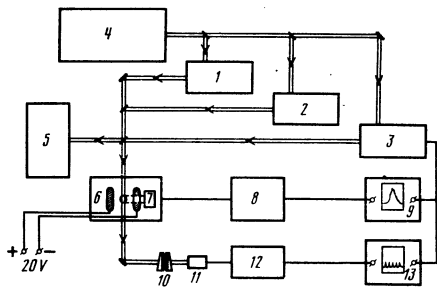


FIG. 3. Schematic diagram of the apparatus: 1), 2), 3) dye lasers; 4) nitrogen laser; 5) spectrograph; 6) vacuum chamber; 7) secondary-electron multiplier; 8) gated storage device; 9), 13) X-Y plotters; 10) Fabry-Perot etalon; 11) photo-diode; 12) dc amplifier.

identify just the states with $L=1$ and thus complete unambiguous classification of autoionizing states.

The apparatus is shown schematically in Fig. 3. The ytterbium atoms were excited in an atomic beam by three dye lasers 1, 2, 3 pumped simultaneously by one nitrogen laser 4. The output power of the dye lasers was of the order of 1 kW, the pulse repetition frequency was 12 Hz, and the width of the emission spectrum was about 1 cm^{-1} . Dye laser beams were directed to a vacuum chamber 6 where an atomic Yb beam was formed by heating metallic ytterbium to 450°C in a crucible with a narrow cylindrical channel. Laser beams intersected the atomic beam in a region between two electrodes, which were subjected to a weak static field $\epsilon = 20 \text{ V/cm}$ used to ensure efficient extraction of ions. After excitation to an autoionizing state, an ytterbium atom ionized spontaneously. The resultant ion passed through a slit in one of the electrodes and were recorded with a secondary-electron multiplier 7. The multiplier signal was averaged by a gated storage element and applied to the Y input of an X-Y plotter 9. The tunable radiation from the third laser passed through a vacuum chamber and was directed to a Fabry-Perot etalon 10, and then to a diode 11; it was recorded by a second X-Y plotter 13 in the form of frequency marks. The plotters were driven synchronously with rotation of a diffraction grating of the laser used in the third stage. The frequency marks provided by the Fabry-Perot etalon were used to determine the relative positions of autoionizing resonances and to estimate their width. The absolute positions of the resonances were found by measuring the emission wavelength of the third laser with a spectrograph 5. The width of the narrow (of the order of 1 cm^{-1} or less) autoionizing states was determined using a tunable dye laser with a line width $0.05\text{--}0.1 \text{ cm}^{-1}$, which was used in the third stage.

4. EXPERIMENTAL RESULTS

In the investigated energy range $0\text{--}15000 \text{ cm}^{-1}$ above the ionization threshold of the Yb atom all four excitation schemes revealed large numbers of autoionizing states of both types: narrow states with a width not exceeding 5 cm^{-1} and wide states with a width $30\text{--}100 \text{ cm}^{-1}$. The excitation cross sections of the narrow states were 1–2 orders of magnitude greater than those

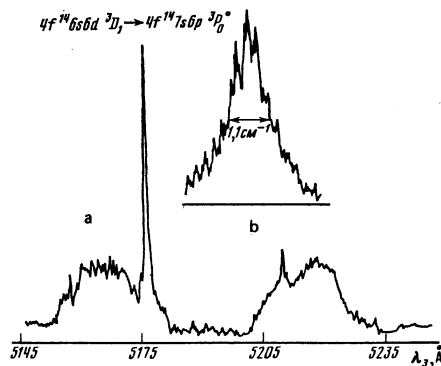


FIG. 4. a) Dependence of the ionic signal on the wavelength of the laser used in the third stage to excite autoionizing states from the intermediate state $6s6d^3D_1$, laser line with $\Delta\nu_3 \approx 1 \text{ cm}^{-1}$. b) Autoionizing resonance of $7s6p^3P_0^o$, recorded with a resolution of $\Delta\nu_3 = 0.1 \text{ cm}^{-1}$.

of the wide states. In our experiments the identification of the autoionizing states was complicated by the fact that, according to our estimates, in the energy range of the autoionizing states of the $7s6p$ configuration, there could be also autoionizing states of the $6p6d$ and $5d7p$ configurations and they should also be narrow. These configurations gave rise to autoionizing states which also have the orbital momentum $L=1$. However, according to the estimates obtained in the one-particle approximation, autoionizing states of the $6p6d$ configuration should be lower, whereas those of the $5d7p$ configuration should be higher than the $7s6p$ states.

In the investigated energy interval there were three energetically separated groups of autoionizing states with $L=1$, which appeared as a result of excitation from both S and D intermediate states. According to our estimates, the middle group of states should belong to the $7s6p$ configuration. We used the method of Sec. 3 to classify these states in accordance with the total momentum J .

Figure 4a shows a part of the ionization spectrum with one of the narrow resonances identified as $7s6p^3P_0^o$. The spectrum was obtained by excitation from the $6s6d^3D_1$ state with laser radiation characterized by a line width of about 1 cm^{-1} . Two wide resonances were clearly associated with the excitation of the $4f$ shell. Similar resonances were also observed in other spectral regions and excitation schemes. Figure 4b shows the autoionization resonance $^3P_0^o$ obtained using a laser in the third stage with the line width $\Delta\nu_3 = 0.1 \text{ cm}^{-1}$.

The experimental results were characterized by a large scatter of the photoionization cross sections of the $6s6d - 7s6p$, $6s8s - 7s6p$ transitions in the third stage. As in the case of autoionization widths, the scatter was due to a redistribution of the oscillator strengths as a result of superposition of almost degenerate states. The intensities of the transitions between the mixed states could differ by one or two orders of magnitude. The transitions in the third stage were formally of the two-electron type. Nevertheless, the majority of them had large photoexcitation cross sections. Estimates (confirmed subsequently by calculations) indicated that the nodes of the orbitals $6s$, $7s$,

and 8s practically coincided in the main electron localization region and this resulted in their strong overlap. Thus, the transitions in question could in fact be regarded as one-particle 6s - 6p and 6d - 6p transitions, and this was why they had large excitation cross sections.

5. THEORETICAL CALCULATION

We shall describe the E electron state of the system by a relativistic equation with the Hamiltonian

$$\sum_i h(r_i) + \sum_{i>j} \left(\frac{1}{r_{ij}Z} + V_{ij} \right), \quad (3)$$

where $h(r_i)$ is the Dirac Hamiltonian for one electron in the Coulomb field of a nucleus and V_{ij} is the Breit electron-electron interaction. This equation allows fully for all the one-electron relativistic effects (apart from radiative corrections). The two-electron relativistic interaction is allowed for to within terms proportional to α^2 . The many-electron equation was solved by the perturbation theory method dividing the Hamiltonian into the following components:

$$H_0 = \sum_i [h(r_i) + V_{el}(r_i)], \quad H_{int} = \sum_{i>j} \frac{1}{r_{ij}Z} - \sum_i V_{el}(r_i). \quad (4)$$

In the zeroth-approximation Hamiltonian H_0 we have included the one-electron central potential V_{el} simulating the electron-electron interaction. This potential is derived so that even the zeroth perturbation theory approximation includes a considerable proportion of the correlational and relativistic effects. In the derivation of V_{el} a heavy reliance is placed on the experimental energy spectrum of the simpler $4f^{14}nl$ system of Yb^+ with one valence electron. In our treatment, we shall assume that

$$V_{el} = V_1 + V_2 + V_3, \quad (5)$$

where V_1 , V_2 , and V_3 approximate, respectively, the potentials of the K shell, L shell, and the remaining shells of the atomic core.

In deriving the potentials of the inner shells V_1 and V_2 we shall use the experience in calculations of the spectra of multiply charged ions.¹⁰ An analytic form of the potential V_3 is ensured by the Thomas-Fermi behavior of V_{el} in the inner region. The total potential V_{el} simulating the core potential has the correct asymptotes

$$V_{el} \rightarrow \text{const}, \quad dV_{el}/dr \rightarrow 0 \quad \text{as } r \rightarrow 0, \quad V_{el} \rightarrow N/rZ \quad \text{as } r \rightarrow \infty \quad (6)$$

(N is the number of the core electrons). The correct behavior of the potential V_{el} in the limit $r \rightarrow 0$ is important for the determination of the nodes of the orbitals of the valence electrons and of an electron in the scattering state. As pointed out above, this is needed in the calculation of the autoionization widths of the levels.

The total electron energy of the system is

$$E = E^{(0)} + E^{(1)} + E^{(2)}. \quad (7)$$

Here, $E^{(0)}$ is the energy of the core and $E^{(1)}$ is the sum of the binding energies of the valence electrons (with-out allowance for their interaction). We did not calculate $E^{(0)}$ because this energy is independent of the state of the atom and determines only the general shift

of all the levels. We found the value of $E^{(1)}$ from the experimental data. We calculated only $E^{(2)}$, representing the energy of the interaction of two valence electrons with one another. To within the second-order perturbation theory the contribution of $E^{(2)}$ can be represented in the form of the sum

$$E^{(2)} = E_{dir}^{(2)} + E_{pol}^{(2)}, \quad (8)$$

where $E_{dir}^{(2)}$ is the energy of the direct interaction of two electrons and $E_{pol}^{(2)}$ is the energy of their effective interaction via the polarizable core. The value of $E_{dir}^{(2)}$ can be calculated by one of the methods used in the theory of two-electron systems. The correction to the first-order perturbation theory contributes only to $E_{dir}^{(2)}$. This correction is expressed in terms of the Slater radial integrals, which we calculated here numerically. Higher-order corrections were included effectively as the screening of the core potential by one of the valence electrons. The contribution of the higher-order corrections to $E_{dir}^{(2)}$ was of the order of 5000 cm^{-1} .

The polarization of the core (contribution $E_{pol}^{(2)}$) can be included by the superposition of the states with the electron configurations $4f^{13}n_1l_1n_2l_2n_3l_3$. A symmetry analysis and specific calculations indicate that the superposition of a very small number of states with the excited $4f$ shell makes a considerable contribution to $E_{pol}^{(2)}$. It is known that the polarization of the core can be allowed for effectively by modifying the potential of the interaction of valence electrons with one another.¹² This results essentially in redetermination of the Slater radial integrals in $E_{dir}^{(2)}$. In our case the core polarization reduces considerably the exchange radial integrals. This, in its turn, reduces the degree of mixing of the excited configurations of the valence shell. Thus, the core polarization suppresses superposition of the excited configurations of the valence shell and this naturally simplifies the calculation procedure. We shall attribute this simplification to the properties of the selected zeroth approximation.

The calculation is made, right from the beginning, in the representation of the jj scheme of the coupling between the one-electron momenta. The transition to the real scheme is made, as usual, by diagonalization of the energy matrix.

We calculated the autoionization width for the states located above the ionization threshold. The calculations were made using Eq. (1). Technical details of the calculation were described earlier.¹³

Table I gives the results of a numerical calculation of

TABLE I. Energies of singly excited states of Yb atom measured from $4f^{14}$ core energy.

Configuration	J	$E_{\text{calc}}, \text{cm}^{-1}$	$E_{\text{exp}}, \text{cm}^{-1}$
$6s^2_{1/2}$	0	-148700	-148710
$6s_{1/2}6p_{1/2}$	0	-131300	-131422
	1	-130600	-130718
$6s_{1/2}6p_{3/2}$	1	-123200	-123642
	2	-128900	-129000
$6s_{1/2}5d_{3/2}$	1	-124800	-124221
	2	-124100	-123958
$6s_{1/2}5d_{5/2}$	2	-122600	-121032
	3	-123800	-123439

TABLE II. Energies of doubly excited states of Yb atom measured from $4f^{14}$ core energy.

Configuration	J	E_{calc}, cm^{-1}	E_{exp}, cm^{-1}	Configuration	J	E_{calc}, cm^{-1}	E_{exp}, cm^{-1}
$6p_{3/2}^2$	0	-106700	-106273	$6p_{1/2}5d_{3/2}$	3	-96300	-
$6p_{3/2}^2$	2	-92000	-	$6p_{1/2}5d_{3/2}$	4	-106200	-
$6p_{3/2}^2$	2	-98700 ***	-100888 *	$5d_{3/2}^2$	0	-98100 ***	-
$6p_{1/2}6p_{3/2}$	1	-105400	-104900	$5d_{3/2}^2$	2	-103400	-1010 * *
$6p_{1/2}6p_{3/2}$	2	-103200	-103950	$5d_{3/2}^2$	0	-96100	-
$6p_{1/2}5d_{3/2}$	1	-107700	-	$5d_{3/2}^2$	2	-97000	-
$6p_{1/2}5d_{3/2}$	2	-107500	-	$5d_{3/2}^2$	4	-88100	-
$6p_{1/2}5d_{3/2}$	2	-100700	-	$5d_{3/2}^2$	1	-98000 ***	-
$6p_{1/2}5d_{3/2}$	3	-111900	-	$5d_{3/2}5d_{3/2}$	2	-99400	-99463 **
$6p_{1/2}5d_{3/2}$	0	-102000	-	$5d_{3/2}5d_{3/2}$	3	-103000	-103247 **
$6p_{1/2}5d_{3/2}$	1	-101400	-	$5d_{3/2}5d_{3/2}$	4	-102400	-
$6p_{1/2}5d_{3/2}$	2	-91400	-	$7s_{1/2}6p_{3/2}$	0	-88900	-
$6p_{1/2}5d_{3/2}$	3	-103900	-	$7s_{1/2}6p_{3/2}$	1	-88700	-
$6p_{1/2}5d_{3/2}$	1	-94900	-	$7s_{1/2}6p_{3/2}$	1	-85100	-
$6p_{1/2}5d_{3/2}$	2	-111800	-	$7s_{1/2}6p_{3/2}$	2	-88100	-

* Identified by a question mark in Ref. 11.

** In Ref. 11 these levels are attributed to the $4f^{13}6s6p5d$ configuration.

*** The calculation accuracy is insufficient to regard these as autoionizing.

the energies E of singly excited states of the ytterbium atom found allowing for the higher corrections in perturbation theory. We can see that the agreement with the experimental results of Ref. 11 is good. The calculated and experimental values agree to within $\pm 500 cm^{-1}$.

Table II gives the numerical results for the energies of the doubly excited states of Yb considered here. It also compares them with the experimental values of the energies.¹¹ However, we must bear in mind that this is a nominal comparison. The states lie within the same energy range as the $4f^{13}n_1l_1n_2l_2n_3l_3$ states. Therefore, our classification may differ from that adopted in Ref. 11. For example, the theoretical results for the states $4f^{14}5d_{3/2}5d_{5/2}$ ($J = 2, 3$) agree better with the energies adopted in Ref. 11 for the $4f^{13}6s6p5d$ ($J = 2, 3$) states. The difference is greater for the two states identified by "?" in Ref. 11. The calculated widths of the autoionizing states are listed in Table III. These widths range from a few hundredths to a few reciprocal centimeters. Such a large scatter of the widths is due to superposition of almost degenerate autoionizing states. This superposition is known to result in a considerable redistribution of the decay probability.

The widths of the doubly excited states of the Yb atom are 2-3 orders of magnitude less than the widths of the autoionizing states of the He atom, although the

TABLE III. Widths of autoionizing states of Yb atom with doubly excited valence shell.

Configuration	J	Term	Γ, cm^{-1}	Configuration	J	Term	Γ, cm^{-1}
$6p_{3/2}^2$	0	1S_0	5.40	$5d_{3/2}^2$	2	3P_2	0.40
$6p_{1/2}5d_{3/2}$	2	$^1D_2^0$	0.20	$5d_{3/2}^2$	4	1G_4	0.90
$6p_{1/2}5d_{3/2}$	1	$^1P_1^0$	5.70	$7s_{1/2}6p_{3/2}$	0	$^3P_0^0$	0.70
$6p_{1/2}5d_{3/2}$	3	$^1F_3^0$	1.60	$7s_{1/2}6p_{3/2}$	1	$^3P_1^0$	3.00
$5d_{3/2}^2$	0	3P_0	0.01 *	$7s_{1/2}6p_{3/2}$	1	$^1P_1^0$	1.80
$5d_{1/2}5d_{3/2}$	1	3P_1	0.0001 **	$7s_{1/2}6p_{3/2}$	2	$^3P_2^0$	0.70
$5d_{3/2}^2$	0	1S_0	3.30				

*) The calculation is insufficient to regard these states as autoionizing.

binding energies and the dimensions of the electron orbitals participating in the decay process are of the same order of magnitude for both cases. We can attribute this effect, as pointed out earlier, to the occurrence of multiple oscillations of the wave functions in the main electron localization region. We shall assume that this situation is typical of the valence shells of complex atoms.

It should be pointed out that the precision of the calculations does not allow us to conclude reliably whether the states identified by three asterisks in Table II are of the autoionizing type. One of these states, $5d_{3/2}5d_{5/2}$ ($J = 1$), has an anomalously small width ($0.0001 cm^{-1}$). If this state is indeed autoionizing, then its anomalously small width can be explained by the fact that the decay of the state is forbidden in the nonrelativistic limit. Clearly, the state should be characterized by a large quantum yield in radiative decay.

6. COMPARISON OF THE THEORY WITH EXPERIMENT. CONCLUSIONS

Table IV lists the experimentally determined and calculated values of the energies and widths of autoionizing states of the $7s6p$ configuration. The positions of the levels are calculated from the $6s^2$ ground state of Yb. A comparison shows that the agreement between the theory and experiment is good. In the case of the $7s6p^3P_0^0$ state the difference between the calculated and experimental values is $670 cm^{-1}$. This corresponds to a precision of about 1% in the determination of the energy of these states. In all other cases the agreement between the level positions is even better.

The experimental and theoretical values of the widths of the autoionizing levels can sometimes differ by a factor of 2-3 (Table IV). This inaccuracy is due to the approximation employed in the calculation of the radial integrals used to determine the widths of autoionizing states.

Application of the method of multistep photoionization of atoms by laser radiation is very promising for the investigation of autoionizing states since it makes it possible to classify practically unambiguously the recorded autoionizing states.

An analysis of autoionizing states of the many-electron Yb atom with the external $6s^2$ shell shows that this complex atom has narrow autoionizing states which appear as a result of double excitation of the valence shell. Their width is two or three orders of magnitude

TABLE IV. Energies*) E and widths T of $7s6p$ configuration states of Yb atom.

Term	Calculation		Experiment	
	E, cm^{-1}	Γ, cm^{-1}	E, cm^{-1}	Γ, cm^{-1}
$^3P_0^0$	59800	0.70	59130.5	1.2
$^3P_1^0$	60000	3.00	60428.7	0.95
$^3P_2^0$	62800	0.70	62529.1	1.6
$^1P_1^0$	63600	1.80	63655.8	2.6

*) Energies measured from the energy of the ground state $4f^{14}6s^2^1S_0$ of the Yb atom.

less than the width of lower autoionizing states of the He atom and of autoionizing states which appear as a result of excitation of the $4f$ shell. The smallness of the width of these states is associated with multiple oscillations of the wave functions of one-particle states in the main interaction region, which reduces the probability of ionization decay. This is typical of autoionizing states of the valence shells of the heavy atoms.

A good agreement is obtained between the experimental results and those found by numerical (theoretical) calculation of the positions of narrow autoionizing states in the spectrum of the Yb atom near the ionization threshold, which confirms the correctness of the selected experimental method for investigating these states.

The theoretical approach adopted above is equally suitable for the investigation of other many-electron systems, particularly of atoms with three valence electrons.

¹G. I. Bekov, V. S. Letokhov, O. I. Matveev, and V. I. Mishin, *Pis'ma Zh. Eksp. Teor. Fiz.* **28**, 308 (1978) [*JETP Lett.* **28**, 283 (1978)].

²R. F. Stebbings, F. B. Dunning, and R. D. Rundel, in: *Atomic Physics 4* (Proc. Fourth Intern. Conf. on Atomic Physics, Heidelberg, 1974), Plenum Press, New York, 1975, p. 713.

³J. J. Wynne and J. P. Hermann, *Opt. Lett.* **4**, 106 (1979).

⁴J. A. Paisner, R. W. Solarz, L. R. Carlson, C. A. May, and S. A. Johnson, Preprint UCRL-77537, Lawrence Livermore Laboratory, November, 1975.

⁵E. F. Worden, R. W. Solarz, J. A. Paisner, and J. G. Conway, *J. Opt. Soc. Am.* **68**, 52 (1978).

⁶G. I. Bekov, E. P. Vidolova-Angelova, V. S. Letokhov, and V. I. Mishin, *Laser Spectroscopy IV* (Proc. Fourth Intern. Conf., Rottach-Egern, West Germany, 1979), Springer Verlag, Berlin, 1979, p. 283.

⁷V. S. Letokhov, *Nature (London)* **277**, 605 (1979).

⁸L. N. Ivanov, *Opt. Spektrosk.* **38**, 31 (1975) [*Opt. Spectrosc. (USSR)* **38**, 16 (1975)].

⁹C. E. Moore, *Atomic Energy Levels as Derived from the Analyses of Optical Spectra* (Nat. Bur. Stand. Circ. No. 467), Vol. 1, National Bureau of Standards, Washington, D. C., 1949.

¹⁰L. N. Ivanov and L. I. Podobedova, *J. Phys. B* **10**, 1001 (1977).

¹¹W. C. Martin, R. Zalubas, and L. Hagan, *Atomic Energy Levels as Derived from the Analyses of Optical Spectra* (Nat. Bur. Stand. Circ. No. 467), The Rare-Earth Elements, National Bureau of Standards, Washington, D. C., 1978.

¹²C. Bottcher and A. Dalgarno, *Proc. R. Soc. London Ser. A* **340**, 187 (1974).

¹³L. N. Ivanov, E. P. Ivanova, U. I. Safronova, and I. A. Shavtvalishvili, *Opt. Spektrosk.* **44**, 12 (1978) [*Opt. Spectrosc. (USSR)* **44**, 6 (1978)].

Translated by A. Tybulewicz

Polarization and angular distribution of Cherenkov and transition radiations in the field of a strong electromagnetic wave

I. G. Ivanter and V. V. Lomonosov

I. V. Kurchatov Institute of Atomic Energy, Moscow

(Submitted 29 May 1980)

Zh. Eksp. Teor. Fiz. **80**, 879-890 (March 1981)

An analysis is made of the influence of an external electromagnetic field on Cherenkov and transition radiations. It is shown that considerable changes appear in the angular and spectral distributions of these radiations. Strong polarization may be acquired and fairly hard photons with energies of several kiloelectronvolts may be emitted.

PACS numbers: 41.70. + t

1. Quantum theory of transition radiation in the absence of an external electromagnetic field is given in Ref. 1. We shall consider Cherenkov and transition radiations of a longitudinally polarized lepton (electron, muon) moving from medium 1 to medium 2 (Fig. 1) whose permittivities are ϵ_1 and ϵ_2 . We shall use as independent solutions of the wave equation those which correspond to the case when the principal wave (identified by the thick line in Fig. 1) can be produced, as in Ref. 1, by refraction or reflection of auxiliary waves.

Case a represents a situation in which radiation enters

medium 1, whereas case b corresponds to a situation when radiation enters medium 2. The radiating particle moves from medium 1 to medium 2. We shall consider only the situation when we can ignore an electromagnetic (laser) wave reflected from the interface between the two media, i.e., when the reflection coefficient at the laser frequency is low. We shall study transition radiation at frequencies other than the laser frequency.

The matrix element for a transition of a fermion from a state φ_b to a state φ_b' accompanied by the emission of a photon with a 4-momentum $f = (\omega, \mathbf{f})$ and a polariza-